

Fatigue Properties of Superalloy IN 713LC and Relation to Microstructure

Ludvík KUNZ^{1*}, Petr LUKÁŠ¹, Radomila KONEČNÁ²

¹*Institute of Physics of Materials, Academy of Sciences of the Czech Republic, Žitkova 22, 616 62 Brno, Czech Republic*

²*University of Žilina, Univerzitná 1, Žilina, Slovak Republic*

Received 01 June 2008; accepted 29 June 2008

The paper presents experimental results of determination of high-cycle fatigue life of IN 713LC at 800 °C in air at stress symmetrical loading and under action of tensile mean stresses. The influence of small cyclic component superimposed on high tensile mean stress was experimentally determined. Three nominally identical casts were investigated. Fractographic observation has been made with the aim to reveal the fatigue crack initiation place, its kind and relation to the casting defects and material microstructure. The observed high scatter of lifetime data has been correlated with the defect size and defect distribution and type of crack initiation. The extreme value statistics for inclusion size originally developed by Murakami for small defects in material has been adopted and tested for this particular case.

Keywords: IN 713LC, high-cycle fatigue, casting defects, extreme value statistics.

1. INTRODUCTION

Nickel base cast superalloy IN 713 and its low carbon variant IN 713LC are alloys employed in the aircraft gas turbine market. In spite of the application of IN 713 since the mid-1950s, leading European industrial companies are still interested in the more reliable characterization of the high temperature high-cycle fatigue (HCF) properties [1]. The chemical composition of this superalloy is relatively simple, the material costs are relatively low and the cast components can be used in as cast state [2]. Because the casting defects substantially reduce the fatigue strength, “defect free” components are required in engineering practice. In reality it means that the defect size is not allowed to exceed a critical size given by the resolution limit of defectoscopic methods, which is usually some tenths of a millimetre.

One of the important mechanical properties at high temperatures is the high-cycle fatigue resistance. The high temperature mechanical performance depends critically on microstructure. It can dramatically vary according to the casting conditions. The problem is that even when nominally the same material and casting conditions are applied, the variations in microstructure of different batches may be substantial and they can result in appreciable differences of mechanical properties. It has been shown long time ago that the fineness of cast microstructure influences the creep behavior in a substantial way [3]. However, similar studies related to the influence of microstructure on fatigue properties are not available, at least in scientific electronic databases and in available open literature.

The aim of this work was to investigate the HCF strength of IN 713 LC superalloy both at symmetrical loading with stress ratio $R = -1$ and at presence of tensile mean stresses. The influence of microstructure on fatigue crack initiation and fatigue life was studied.

2. EXPERIMENTAL

Conventionally cast cylindrical rods of 20 mm in diameter and of 100 mm in length were provided by the company PBS Velká Bíteš a.s. Three nominally identical batches denoted as batch 1, 2 and 3 were cast within two years. All rods were controlled by conventional X-ray non-destructive defectoscopy and were found “defect free”, which means that the defect size was below the resolution limit of the method used, which is about 0.5 mm.

Cylindrical button-end specimens of 5 mm and 6 mm in diameter and with 35 mm long gauge length were machined from the rods. The final operation was a fine grinding.

The grain size determined by means of linear intercept method on axial sections of gauge length of specimens manufactured from all these batches was (3 ± 0.5) mm. Grains were characterized as equiaxial.

The cast microstructure is dendritic in nature, Fig. 1. Dendrites with long primary arms can be observed. Though nominally identical casting processes were applied by production of particular batches, the dendrite structure differs. Differences of smaller extend were found also between rods from the same batch.

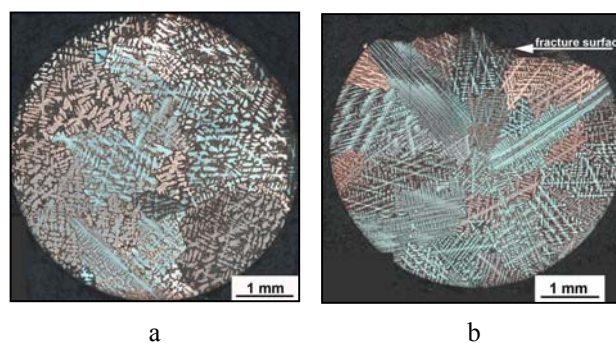


Fig. 1. Dendritic structure. Transversal sections of the gauge length of specimens. a – batch 1, b – batch 2. Fracture profile created by intersection of the plane of the metallographic section by fracture surface can be seen

*Corresponding author. Tel.: + 420-549-246327; fax: + 420-541-218657. E-mail address: kunz@ipm.cz (L. Kunz)

The microstructure as observed under higher magnification on longitudinal axial sections of the gauge length of specimens is shown in Fig. 2. Similarly to the structure shown in Fig. 1 there is a clear difference in the fineness of cast microstructure of both batches.

Dendritic regions with regular γ/γ' microstructure, interdendritic areas with small cavities, casting defects, carbides and colonies of large and irregular γ' particles can be seen on scanning electron micrographs, Fig. 3, a. The dendritic regions are characteristic with very fine regular γ/γ' microstructure. An example of a colony of irregular γ' particles embedded in the fine γ/γ' microstructure is shown in Fig. 3, b.

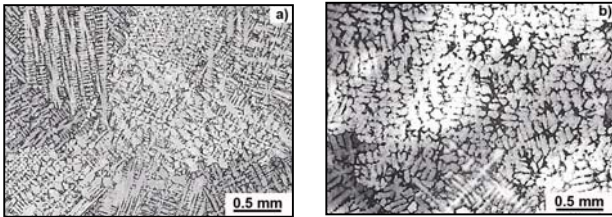


Fig. 2. Dendritic structure. Longitudinal sections of the specimen gauge length: a – batch 1, b – batch 2

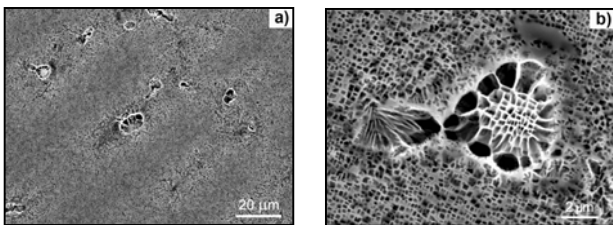


Fig. 3. Microstructure as observed by scanning electron microscopy: a – dendritic and interdendritic regions, b – colony of irregular γ' particles embedded in the fine γ/γ' structure

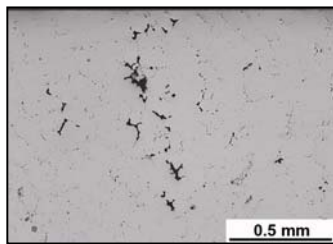


Fig. 4. Casting defects at the longitudinal axial section of the specimen gauge length, batch 2

Fatigue testing was performed in HCF region by means of 100 kN resonant testing systems operating under controlled load. The mean stress has been controlled since the start of heating. It was kept at zero level as long as the specimen was not at the desired temperature for at least two hours. Then the chosen non-zero mean stress was set up during several seconds. After that the resonant system was switched on. The full stress amplitude was reached during several hundreds of loading cycles. The frequency of sine loading was of about 100 Hz and was slightly dependent on the stiffness of the specimen. The heating of specimens was performed in an electric resistance furnace. Tests were run in laboratory air. The long-term stability of temperature of specimen gauge length was within $\pm 1^\circ\text{C}$.

The temperature gradient at the central part of the gauge length was smaller than $3^\circ\text{C}/\text{cm}$.

Structural defects, such as porosity or casting defects are generally known to be responsible for scatter of fatigue life data. Statistical extreme value theory has been proved to be useful for evaluation of fatigue limit. The results can be used also for prediction of fatigue lifetime of large components and for the control of manufacturing process [4]. Fig. 4 shows the casting defects on a longitudinal axial section of the specimen gauge length of material from batch 2. In order to perform statistical evaluation of casting defect distribution inspection of polished surface was carried out by means of light microscopy. Image analysis software was used to determine the size of casting defects. The sampling for determination of the largest extreme value distribution was performed on inspection areas $S_0 = 1.827 \text{ mm}^2$. The size of defects was determined in terms of square root area. The largest defect area $(\text{area}_{\text{max}})^{1/2}$ was determined on 25 places chosen on a polished axial section of a part of the specimen gauge length of $5 \text{ mm} \times 20 \text{ mm}$ dimension. The results were processed by the largest extreme value distribution method [4] and presented in terms of Gumbel plots.

3. RESULTS

The experimentally determined S-N data in the HCF region for load symmetrical cycling and for loading with tensile mean stresses of 300 MPa and 500 MPa can be seen in Fig. 5. Full open or half-open points distinguish results obtained on particular batches. Tensile mean stress reduce the fatigue strength in the high-cycle fatigue region. Though there is a considerable scatter of data, it is obvious that the fatigue life for tensile mean stresses 300 MPa and 500 MPa is substantially shorter than that for symmetrical loading for given stress amplitude. The dashed line in Fig. 5 corresponds to the S-N curve for symmetrical cycle experimentally determined in the broad stress amplitude interval covering also low cycle fatigue region [5, 6].

The dependence is described by the equation

$$\sigma_a = 1208 N_f^{-0.133}, \quad (1)$$

where σ_a is in MPa. The equation gives for the 10^7 cycles to fracture the endurance limit 142 MPa. The corresponding value for mean stress of 500 MPa is three times lower.

Though there is a considerable scatter of experimental points in Fig. 5, differences in the fatigue strength of individual batches can be recognized. For constant stress amplitude the lifetime of specimens from the batch 1 is higher than that of batches 2 and 3.

Fatigue loading with high tensile mean stresses results in cyclic creep. The time to fracture of a specimen loaded at temperature of 800°C and sustained stress of 500 MPa is nearly 6 hours, Fig. 6. Superposition of small stress amplitudes up to 50 MPa does not result in a decrease of time to fracture, though the maximum stress in cycle increases. The dependence is non-monotonous. Substantial decrease of lifetime is observed not until the stress amplitude exceeds 50 MPa.

Two types of fracture were observed. For pure creep loading, i. e. for loading with the mean stress only or for very small stress amplitudes the typical fracture surface is

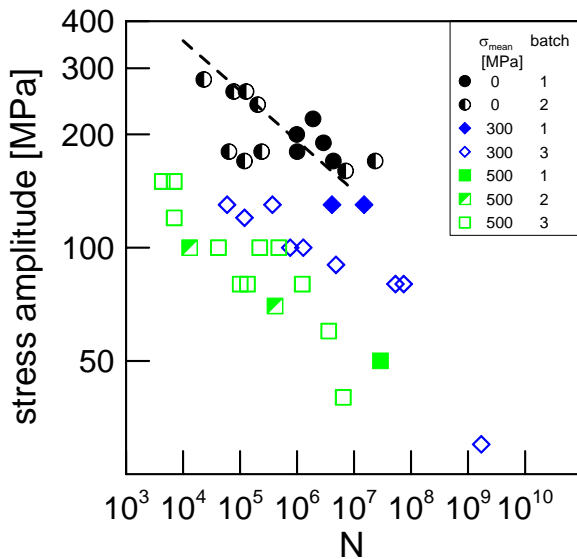


Fig. 5. S-N data of three batches of IN 713 LC for stress symmetrical loading and loading with tensile mean stress

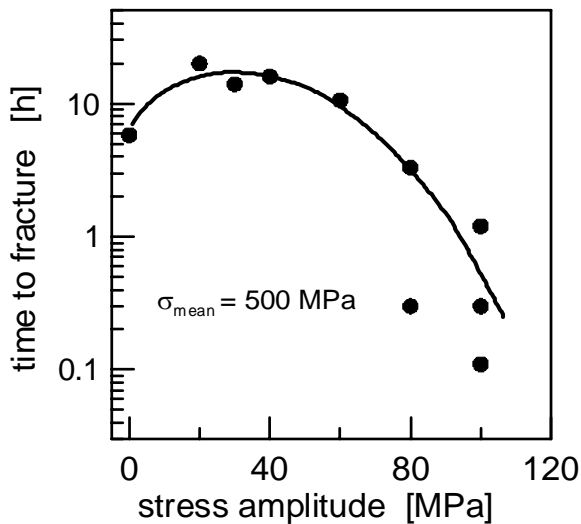


Fig. 6. Dependence of time to fracture on stress amplitude superimposed on tensile mean stress 500 MPa

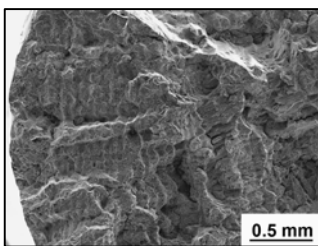


Fig. 7. Fracture surface of crept specimen

shown in Fig. 7. The fracture is of a ductile type. The dendrite morphology can be often well seen on the fracture surface.

For cyclic loading with stress amplitudes corresponding to or higher than the maximum on the time to fracture vs. stress amplitude curve, Fig. 6, two types of fatigue crack initiation were observed. The first one is associated with casting defects. An example can be seen in Fig. 8. The origin of the fatigue crack is located on large casting

defect in material interior. The fatigue crack propagated internally by non-crystallographic manner, macroscopically perpendicular to the principal stress. Typical “fish eye” can be observed on the fracture surface. When the crack reaches the specimen surface, the crack propagation changes due to the influence of air and the fracture surface exhibits different appearance. The crack front corresponding to the transition from fatigue propagation to the final rupture can be seen in Fig. 8 too.

The second type of fatigue crack initiation is related to the development of crystallographic facets. They have mirror appearance at low magnification. An example is shown in Fig. 9. An arrow indicates the facet with the area of nearly 1 mm^2 . Very often systems of parallel crystallographic facets inclined mutually at high angles can be found on the fracture surface. An example is shown in Fig. 10. At higher magnification decohesion between crystallographic facets can be seen. Arrows in Fig. 11 mark this decohesion.

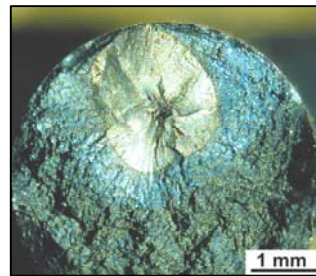


Fig. 8. Crack initiation on a large casting defect



Fig. 9. Crystallographic crack initiation

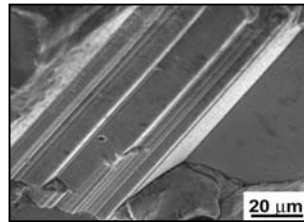


Fig. 10. Two systems of parallel of crystallographic facets on the fracture surface

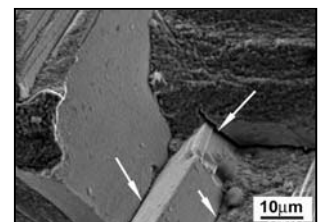


Fig. 11. Decohesion between facets

Results of evaluation of casting defect distribution on polished surface are shown in Fig. 12. Two data sets of extreme values of casting pore size, $A^{1/2} \equiv (\text{area}_{\text{max}})^{1/2}$ determined by means of optical microscopy and processed by image analysis software for are presented. The dependences are linear, which means that the distribution of casting pores obey the extreme value statistics.

4. DISCUSSION

The experimental results confirm the general rule that the application of tensile mean stress decreases the fatigue strength. Indeed, according to the eq. (1) the endurance limit of IN 713LC for 10^7 cycles is 142 MPa, whereas for the mean stress 300 MPa and the batch 3 the value of 80 MPa can be derived from Fig. 5. For the mean stress 500 MPa the endurance limit is three times lower than for symmetrical loading and equal to 50 MPa.

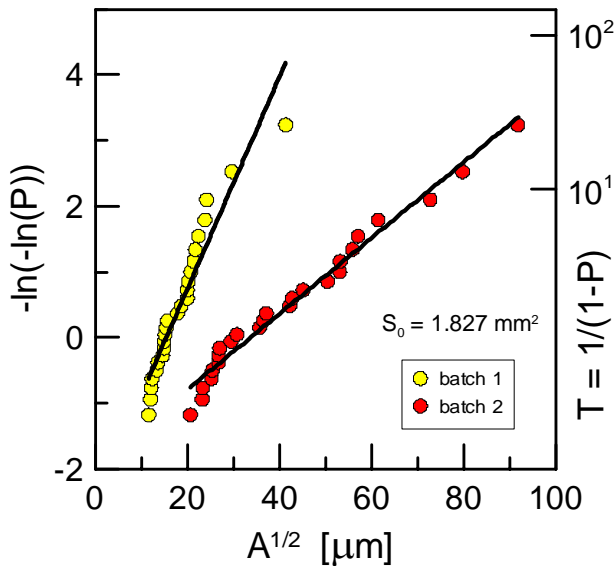


Fig. 12. Extreme value statistics for casting defects in the batch 1 and 2

When the mean stresses are high and cyclic creep does play an important role, it is advantageous to characterize the strength of material in terms of the dependence of time to fracture on the stress amplitude. This representation enables to involve pure creep into diagram, i. e. loading at the sustained load. The dependence presented in Fig. 6 brings evidence that application of small vibrations on highly stressed material which creeps is not dangerous from the point of view of the lifetime. In other words, small vibrations superimposed on mean stress are harmless, though the maximum stress in a loading cycle increases. For the particular case shown in Fig. 6 this holds for asymmetrical loading in the range of R ratio $R \in (0.8; -1)$. Stress ratio R is defined as $R = \sigma_{\min}/\sigma_{\max}$. This observation on IN 713 LC corresponds to the very old experimental results showing a “nose” on the $\sigma_a - \sigma_{\text{mean}}$ dependence, i. e. on the constant fatigue life diagram of IN 80 [7]. Similar observation was reported for smooth and notched CMSX-4 and CM 186LC singlecrystalline superalloys [8].

The serious problem of all cast materials, including superalloys, is existence of casting defects which can substantially reduce the fatigue strength. The problem is most pronounced just in HCF region. The reliable prediction of fatigue strength requires the possibility to evaluate the influence of defects and to predict their largest size in a component.

The results shown in Fig. 12 bring evidence that there are substantial differences in particular batches of IN 713LC as regards the casting defect distribution, though the batches are considered from the point of view of engineering technology as nominally identical. The trend of both dependences in Fig. 12 is linear, which means that the casting defects follow the lognormal distribution. The Gumbel plot can be used for prediction of largest defect in given volume, using the return period $T = 1/(1/P)$ [4]. From the slope of the curves it follows that the specimens manufactured from the batch 2 will contain larger defects than specimens manufactured from the batch 1. The largest expected casting defect size in the same volume of batch 2 is three times larger than that in the material from the batch 1. The experimentally determined fatigue strength is

qualitatively in coincidence with this fact. The lifetime of specimens from the batch 1 is generally higher than that of batch 2.

The plot in Fig. 12 enables to predict the maximum casting defect size in the axial section of the specimen. The return period T for the axial section of the whole gauge length is equal to 96, which yields the largest defect size of about $A^{1/2} = 110 \mu\text{m}$ for the batch 2 μm and $40 \mu\text{m}$ for the batch 1. These predicted values are small compared to the dimensions of casting defects observed at the fracture surfaces at the crack initiation site. An example of a large casting defect on the fatigue fracture surface at the site of crack initiation is shown in Fig. 13. The individual voids are small, but they form a large mutually interconnected cluster. The diameter of a whole cluster is nearly 0.5 mm. The applied method for determination of the extreme values of casting defects based on the examination of the area of individual defects on the polished sections, Fig. 4, does not take into account the clustering. Voids in clusters are obviously interconnected. From the point of view of fatigue crack initiation the influence of the whole cluster has to be taken into account. The stress concentrations of individual voids in a cluster interfere and result in easier fatigue crack initiation.

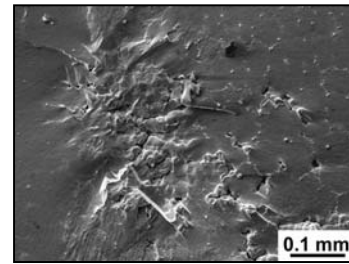


Fig. 13. Large casting defect in material from batch 2 in the site of crack initiation

The experimentally observed large scatter of S-N data both at symmetrical loading and loading with mean stress can be rationalized on the basis of two effects. (i) Fatigue strength of a given volume is related to the size of maximum casting defect. Variability in this size, which increases with increasing volume results in the scatter of the experimental S-N data. (ii) Variability in crystallographic crack initiation and its relation to the microstructure. In the case of crystallographic crack initiation and formation of crystallographic facets the dimension of active planes is of the order of grain size. The decohesion along this planes, which is documented in Fig. 11, results in formation of internal cracks which may substantially differ by size. That is why the fatigue lifetime of particular specimens can vary substantially, according to the particular structural details. The relation between initiation of crystallographic facets and casting defects is not entirely clear. In some cases there seems to be direct relation: systems of facets are observed close to casting defect at the site of fatigue crack initiation. On the other hand, crystallographic facets often cut small pores without any sign of plastic deformation in their vicinity. This indicates, that the development of facets may not be directly related to the stress concentration effect of casting defects. Petre nec et al. [9] studied the localization of the cyclic plastic

deformation in IN 713LC in a broad temperature interval. They observed highly inhomogeneous dislocation arrangement and development of dislocation rich slabs in the form of thin bands and ladder-like bands parallel to the $\{111\}$ crystallographic planes passing through the γ matrix and γ' precipitates. Formation of persistent slip bands passing the γ/γ' microstructure along the $\{111\}$ crystallographic planes which may be the nuclei of fatigue cracks were observed also in Ni-base single crystals CMSX-4 loaded at high mean stress [10]. Persistent slip bands represent weakened planes which are suitable for decohesion. The decohesion results in development of internal cracks, which may substantially differ in size and subsequently result in scatter of fatigue lifetime.

5. CONCLUSIONS

1) Increasing tensile mean stress results in a decrease of fatigue lifetime of cast IN 713LC alloy at 800 °C in high cycle fatigue region.

2) Application of small cyclic stress component with 100 Hz frequency on material exposed to high tensile mean stress does not reduce the lifetime. The time to fracture even increases with increasing stress amplitude. The reverse of this trend is associated with the change of the fracture mechanism from creep dominated to fatigue initiated.

3) Casting defects cause considerable scatter of S-N data. Two different types of crack initiation were observed. Initiation on large casting defects with subsequent non-crystallographic crack propagation and crystallographic initiation resulting in development of large crystallographic facets.

4) The high scatter of S-N data is related to the presence of casting defects and to the structural sensitivity of decohesion along the $\{111\}$ crystallographic planes.

5) The application of the largest extreme value distribution method to statistical description of maximum equivalent casting defect differentiate among particular batches of otherwise nominally identical IN 713LC superalloy. The qualitative evaluation is in agreement with the mutual relation of fatigue strength of individual batches. However, the troublesome fact in the prediction of the largest casting defects is the clustering of casting pores,

which were not taken into account and which have to be treated to reach more reliable prediction.

Acknowledgments

This work was supported by the project 1QS200410502 of the Academy of Sciences of the Czech Republic and by the project FT/TA4/023, Ministry of Industry and Trade of the Czech Republic. This support is gratefully acknowledged.

REFERENCES

1. Information on http://ec.europa.eu/research/transport/projects/article_6513_en.html.
2. **Hakl, J., Vlasák, T., Lapin, J.** Creep Behaviour and Microstructural Stability of Cast Nickel Based Superalloy IN 792 5A *Kovove Mater* 45 2007: pp. 177 – 188.
3. **Quested, P. N., Osgerby, S.** Mechanical Properties of Conventionally Cast, Directionally Solidified and Single-Crystal Superalloys *Materials Science and Technology* 2 1986: pp. 461 – 475.
4. **Murakami, Y.** Metal Fatigue: Effects of Small Defects and Nonmetallic Inclusions. Elsevier, 2002.
5. **Obřtlík, K., Man, J., Polák, J.** Room and High Temperature Low Cycle Fatigue of Inconel 713 LC *In: Proc. of Euromat 2001 Conference* Rimini 2001, AIM Milano 2001.
6. **Kunz, L., Lukáš, P., Mintách, R., Konečná, R.** High Cycle Fatigue of IN 713 LC *In: Proc. of ECF16 Conference* Brno, September 2008 (to be published).
7. **Forrest, P. G.** Fatigue of Metals. Oxford, Pergamon Press, 1962.
8. **Lukáš, P., Kunz, L., Svoboda, M.** High-Temperature Ultra-High Cycle Fatigue Damage of Notched Single Crystal Superalloys at High Mean Stresses *International Journal of Fatigue* 27 2005: pp. 1535 – 1540.
9. **Petrenc, M., Obřtlík, K., Polák, J.** Inhomogeneous Dislocation Structure in Fatigued INCONEL 713LC Superalloy at Room Temperature and Elevated Temperatures *Materials Science and Engineering A* 400 – 401 2005: pp. 485 – 488.
10. **Lukáš, P., Kunz, L., Svoboda, M.** High Cycle Fatigue of Superalloy Single Crystals at High Mean Stress *Materials Science and Engineering A* 387 – 389 2004: pp. 505 – 510.